DOI: 10.1002/chem.200500330

Addition of Nitriles to Alkaline Earth Metal Complexes of 1,2-Bis[(phenyl)imino]acenaphthenes

Igor L. Fedushkin,* Alexander G. Morozov, Oleg V. Rassadin, and Georgii K. Fukin[a]

Dedicated to Prof. Dr. Herbert Schumann on the occasion of his 70th birthday

Abstract: Compounds [Sr(dpp-bian)-(thf)$_4$] (**2**), [Ba(dpp-bian)(dme)$_{2.5}$] (**3**) and [Mg(dtb-bian)(thf)$_2$] (**4**) (dpp-bian = 1,2-bis[(2,6-diisopropylphenyl)-imino]acenaphthene; dtb-bian = 1,2-bis[(2,5-di-*tert*-butylphenyl)imino]acenaphthene) were prepared by reduction of dpp-bian and dtb-bian with an excess of metallic Mg, Sr, or Ba in THF or DME. Reactions of [Mg(dpp-bian)(thf)$_3$], **3**, and **4** with diphenylacetonitrile gave keteniminates [Mg(dpp-bianH)(NCCPh$_2$)(thf)$_2$] (**5**), [Mg(dtb-bianH)(NCCPh$_2$)(thf)$_2$] (**6**), and [Ba(dpp-bianH)(NCCPh$_2$)(dme)$_2$] (**7**), respectively. The reaction of **2** with CH$_3$C≡N in THF gave [{Sr(dpp-bianH)[N(H)C(CH$_3$)C(H)CN](thf)}$_2$] (**8**). The compounds **2**, **3**, **5**–**8** were characterized by elemental analysis, and IR and NMR spectroscopy. Molecular structures of **2**, **3**, **7**, and **8** were determined by single-crystal X-ray diffraction. In contrast to reactions of alkali-metal reagents, magnesium amides, or yttriumalkyls with α-H acidic nitriles, which are accompanied by an amine or an alkane elimination, the reactions of [Mg(dpp-bian)(thf)$_3$] (**1**), **2**, **3**, and **4** with such nitriles proceeded with formation of Mg, Sr, and Ba keteniminates and simultaneous protonation of one nitrogen atom of the bian ligand. The NMR spectroscopic data obtained for complex **5** indicated that in solution the amino hydrogen atom underwent the fast (on the NMR timescale) shuttle transfer between both nitrogen atoms of the dpp-bianH ligand.

Keywords: alkaline earth metals · iminolization · N ligands · nitriles

Introduction

Our research interest focuses on preparation of main-group metal complexes, which may emulate specific reactivity of coordination and organometallic compounds of transition metals. We have found that complex [Mg(dpp-bian)(thf)$_3$] (**1**),[1] which contains dianionic chelating ligand 1,2-bis[(2,6-diisopropylphenyl)imino]acenaphthene (dpp-bian), is highly reactive towards some organic compounds.[2]

In contrast to transition metals,[3] in complexes of Group 1, 2, 13, and 14 metals dpp-bian may act as radical anionic or dianionic ligand,[1,4] and can be chemically reduced or oxidized while still coordinated to the metal. This feature of dpp-bian ligand is correlated to ability of transition metals to change their oxidation state. Several reaction pathways may be expected for metal complexes of dpp-bian dianion (Scheme 1).

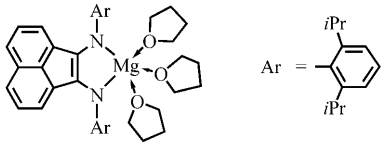

1

Thus, the reaction routes a, c, and d (Scheme 1) took place when **1** was treated with diphenylketone,[2a] R–X[2e,f] (R = Me$_3$Si, X = Cl; R = Et, X = Cl, Br, I), and TEMPO,[2g] respectively. The solvent-induced alkyl radical elimination process, which is opposite to route d, has been observed under treatment of complex [Mg(dpp-bian)$^-$(*i*Pr)(Et$_2$O)] with THF.[5]

Recently we have found that complex **1** easily adds acidic substances, for example, H$_2$O[2c] phenylacetylene,[2b] and enolisable ketones.[2d] These reactions become possible due to the high proton affinity of basic nitrogen atoms in dianionic dpp-bian ligand.

[a] Prof. Dr. I. L. Fedushkin, A. G. Morozov, O. V. Rassadin, Dr. G. K. Fukin
G. A. Razuvaev Institute of Organometallic Chemistry
Russian Academy of Sciences, Tropinina 49
603950 Nizhny Novgorod GSP-445 (Russia)
Fax: (+7) 8312-127-497
E-mail: igorfed@imoc.sinn.ru

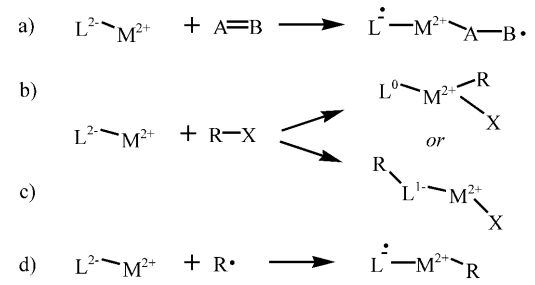

Scheme 1. L = ligand with variable "oxidation state", for example, dpp-bian. M = metal with single oxidation state.

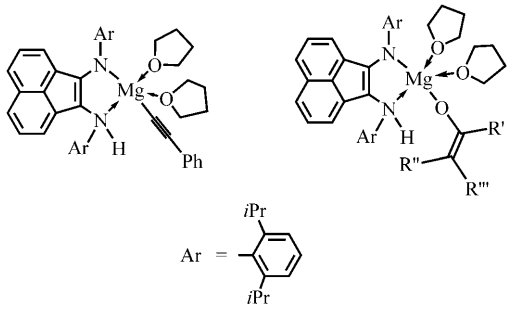

Complex **1** is related to magnesium amides, for example, [Mg(*i*Pr$_2$N)Br] (Hauser base), [Mg(*i*Pr$_2$N)$_2$], and [Mg{(Me$_3$Si)$_2$N}$_2$], which were found to be excellent deprotonating reagents for ketones[6] and phenylacetylene.[7] In 1950 Hauser and co-workers reported deprotonation of acetonitrile using [Mg(*i*Pr$_2$N)Br].[8] In all the reactions of these amides with acidic substances an amine elimination takes place. Since both N atoms of the dpp-bian ligand in **1** are part of a rigid chelating system, the amine elimination becomes impossible for reactions of **1** with acidic substances. In this paper we report the synthesis and characterization of the strontium and barium analogues of **1** as well as their reactions with nitriles.

Results and Discussion

Synthesis of [Sr(dpp-bian)(thf)$_4$] (2) and [Ba(dpp-bian)(dme)$_{2.5}$] (3): Compounds **2** and **3** were prepared by reduction of dpp-bian with an excess of metallic strontium and barium in THF and DME, respectively. Reactions proceeded within few minutes at heating to 60 °C and resulted in the formation of dark red-brown solutions. Separation of these solutions from an excess of metal and evaporation of solvent afforded compounds **2** and **3** as deep red crystalline solids in nearly quantitative yield. In solution and in the solid state **2** and **3** are very sensitive to moisture and air. In the sealed under vacuum capillaries they decompose above 200 °C. Complexes **2** and **3** were characterized by elemental analysis and IR spectroscopy. The molecular structure of **2** was determined by single-crystal X-ray analysis. For **3** the X-ray analysis was also attempted, but due to the poor crystal quality only atom connectivity in the molecule of **3** was established.

Reactions of 1, 2, 3, and [Mg(dtb-bian)(thf)$_2$] (4) with nitriles: Complexes **1**, **2**, and **3**, prepared by reacting the corresponding metals with dpp-bian in THF or DME, were used in situ for the reactions with acetonitrile and diphenylacetonitrile. Addition of one or more equivalents of acetonitrile to a solution of **1** in THF causes an immediate color change from deep green to deep blue. In this case we did not succeed in isolating of product formed. Thus, evaporation of THF afforded deep blue oil, which did not solidify over a period of several days. This oil readily dissolves in toluene, but only an oily residue forms again under evaporation of the solvent in vacuum. Treatment of the oily residue, left after removal of solvent from mother liquor, with Et$_2$O or hexane caused the color to change from blue to violet, hence indicating the formation of the diamine dpp-bian(H)$_2$.[2c]

The color change from green to blue was also observed when **1** was treated with one equivalent of diphenylacetonitrile in THF. The replacement of solvent from THF to benzene gave in this case crystalline [Mg(dpp-bianH)(NCCPh$_2$)(thf)$_2$] (**5**) in 43 % yield. The compound **5** was characterized by elemental analysis, and IR and ^{1}H NMR spectroscopy. Unfortunately, the thin plate-like crystals of **5** obtained from toluene were not suitable for an X-ray crystal structure determination. We decided to use the complex [Mg(dtb-bian)(thf)$_2$] (**4**) (dtb-bian = 1,2-bis[(2,5-di-*tert*-butylphenyl)imino]acenaphthene), which is closely related to **1**, in the reaction with diphenylacetonitrile, thus hoping to get X-ray quality crystals. The reaction of **4** with Ph$_2$CHC≡N proceeded similarly to that of complex **1**. The product of this reaction [Mg(dtb-bianH)(NCCPh$_2$)(thf)$_2$] (**6**) crystallizes from toluene in a form of well-shaped cubic crystals, which revealed still insufficient diffraction under X-ray conditions when a single-crystal structure analysis was attempted. However, compound **6** was well characterized by ^{1}H NMR spectroscopy. The NMR data for **6** are discussed below together with those for **5**. Although the crystal structures of **5** and **6** were not established by X-ray crystallography, one can sketch the structures of **5** and **6** on the basis of ^{1}H NMR spectroscopy data for **5** and **6** and the crystallographic results obtained for related Ba complex.

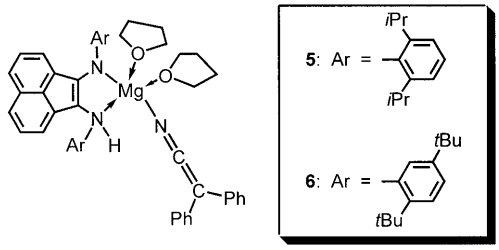

The barium complex **3** reacts with $Ph_2CHC{\equiv}N$ according to the Scheme 2. The reaction product [Ba(dpp-bianH)(N=C=CPh$_2$)(dme)$_2$] (**7**) was isolated in 53% yield as deep blue crystals after crystallization of the crude product from benzene.

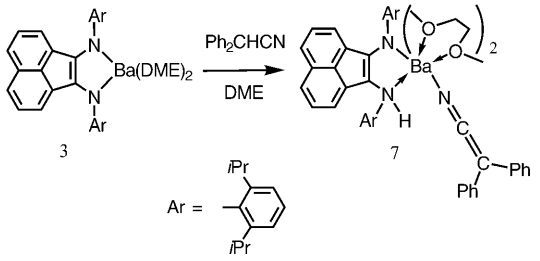

Scheme 2.

The reaction of strontium complex **2** with two equivalents of acetonitrile in THF followed by crystallization from benzene gave [{Sr(dpp-bianH)[N(H)C(CH$_3$)C(H)CN](thf)}$_2$] (**8**) as deep blue crystals in 52% (Scheme 3). As shown by X-ray crystal structure determination dimeric complex **8** consists of crotonitrileamido ligand, which formed through the coupling of acetonitrile molecules. Hydrolysis of **8** in an NMR tube indicated the formation of diamine dpp-bian(H)$_2$[2c] and 3-aminocrotonitrile (Scheme 3). Based on the crystal structure data obtained for **7** one can suggest that the reaction of **2** with $CH_3C{\equiv}N$ proceeds via formation of the strontium complex containing ketenimino ligand, which further reacts with second acetonitrile molecule (Scheme 3).

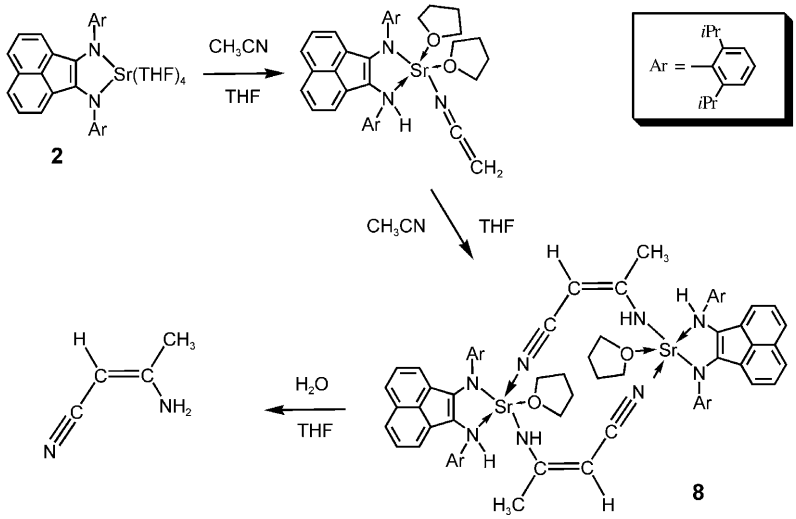

Scheme 3.

The dimerization of acetonitrile to form crotonitrileamido ligand was first achieved 55 years ago by Hauser and co-workers by using [Mg(*i*Pr$_2$N)Br] as a deprotonating agent.[8] The alkali-metal-catalyzed coupling of $CH_3C{\equiv}N$ has been also reported.[9] Later on, Teuben and co-workers used the mono-alkyl yttrium derivative for deprotonation of $CH_3C{\equiv}N$. The product of this reaction, [Y{Me$_2$Si(NCMe$_3$)OCMe$_3$)}$_2$-{N(H)C(CH$_3$)C(H)CN}(thf)]$_2$ is a dimer that consists of two crotonitrileamido ligands bridging two yttrium atoms, as shown by single-crystal X-ray diffraction.[10] The reaction of [Re(CO)$_3$(bpy)(NCCH$_3$)]OTf with sodium hydride in THF proceeds with nucleophilic attack at the nitrile group coordinated to the rhenium(I) center and produces a dinuclear complex in which one bridging crotonitrileamido ligand connects the Re atoms.[11] The keteniminate [Ir(Cp*)(Me$_3$P)Ph-(N=C=CPh$_2$)][12] was prepared by treatment of [Ir(Cp*)-(Me$_3$P)Ph(OH)] with diphenylacetonitrile and catalytic amount of [Ir(Cp*)(Me$_3$P)Ph(OTf)]. Molecular structure of [Ir(Cp*)(Me$_3$P)Ph(N=C=CPh$_2$)] has not been established, but the strong IR band at 2105 cm^{-1} confirmed the presence of ketenimido ligand. In complex **7** the corresponding absorption is shifted to the low wavenumbers and appeared at 2075 cm^{-1}. Deprotonation of $Ph_2HC{-}C{\equiv}N$ with *n*BuLi or Me$_3$M (M = Ga, In) afforded the crystallographically characterized dinuclear complexes [{Li(μ-Ph$_2$C=C=N)(Et$_2$O)$_2$}$_2$] and [{MMe$_2$(μ-Ph$_2$C=C=N)(thf)$_n$}$_2$] (M = Ga, n = 0; M = In, n = 1), respectively.[13] In the lithium complex [{Li(μ-Ph$_2$C=C=N)(Et$_2$O)$_2$}$_2$] the ν(C=C=N) band is shifted down to 2023 cm^{-1}, whereas in [{MMe$_2$(μ-Ph$_2$C=C=N)(thf)$_n$}$_2$] (M = Ga, n = 0; M = In, n = 1) these bands appeared at 2188 (In) and 2167 cm^{-1} (Ga).

^{1}H NMR spectra of the crystallographically characterized complexes **7** and **8** are uninformative due to the broadening of the signals. Useful ^{1}H NMR spectra were obtained for **5** (Figure 1) and **6** in [D$_8$]THF. The solution behavior of **5** is very much alike with those of Mg–enolates[2d] formed from the reactions of **1** with enolisable ketones and the phenylethynyl derivative [{Mg(dpp-bianH)}(C≡CPh)(thf)$_2$],[2b] obtained in the reaction of **1** and PhC≡CH. As indicated by X-ray crystal structure analysis, the molecules of magnesium enolates[2d] and [{Mg(dpp-bianH)}(C≡CPh)(thf)$_2$][2b] posses an unsymmetrical amido/amino structure in the solid state. The same amido/amino pattern of the dpp-bian ligand is found in **7** and **8**. Proceeding on the assumption, that in the solid state complex **5** has molecular structure similar to **7** and this structure will be maintained in solution, the ^{1}H NMR spectrum of **5** should reveal non-equivalence for all aromatic ring protons, as well as for the four methine protons and the eight CH$_3$ groups of the *iso*-propyl substituents of the phenyl moieties of the dpp-bian ligand. However, we expected, that, in analogy to

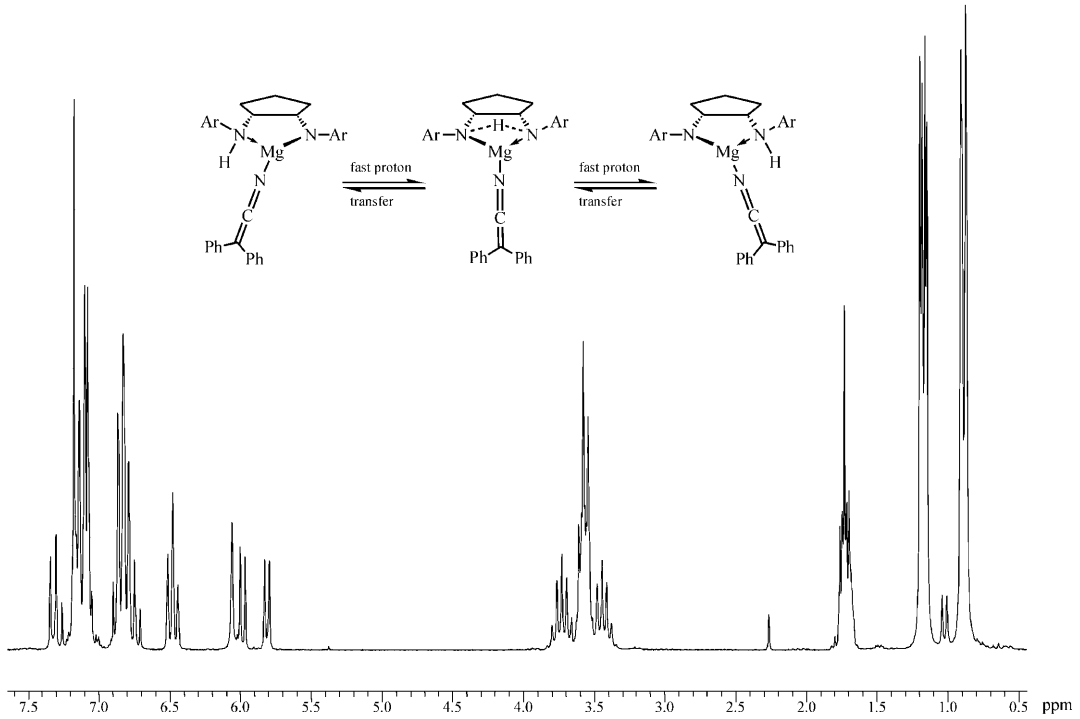

Figure 1. ^{1}H NMR spectrum of **5** in [D_8]THF (200 MHz).

the ^{1}H NMR spectroscopic results obtained for the related Mg–enolates[2d] and for [{Mg(dpp-bianH)}(C≡CPh)(thf)$_2$][2b] molecules **5** in solution will adopt a more symmetrical structure with the amino hydrogen being not fixed at one dpp-bian nitrogen atom, but being delocalized between both nitrogen atoms of the ligand. The fast (on the NMR timescale) shuttle proton transfer between the two N atoms should result in a structure which has a plane of symmetry that bisects the N-Mg-N angle and, thus divides the dpp-bian ligand into two equal parts. This hypothesis is confirmed by the ^{1}H NMR spectrum of **5** in [D_8]THF (Figure 1).

According to our expectation, the ^{1}H NMR spectrum of **5** in [D_8]THF reveals two septets for the methine protons centered at $\delta = 3.73$ and 3.44 ppm. The doublets at $\delta = 1.18$ (6H), 1.16 (6H), and 0.89 ppm (12H) correspond to four pairs of nonequivalent CH_3 groups of *i*Pr substituents. The signal of the delocalized N–H proton appears as a singlet at $\delta = 6.06$ ppm and is shifted to high field relative to those of [{Mg(dpp-bianH)}(C≡CPh)(thf)$_2$] ($\delta = 6.81$ ppm)[2b] and the magnesium enolates ($\delta = 6.42$–6.10 ppm).[2d]

Even assuming that in the case of **6** the proton delocalization also takes place one can expect at least two different spectral pictures due to the different orientations of the 2,5-disubstituted phenyl rings (Figure 2). Both, the *syn* and *anti* orientations in the dtb-bian ligand were found in the metal complexes. For instance, in the crystalline state the magnesium complex [Mg(dtb-bian)(thf)$_2$][4c] revealed an *anti* orientation, whereas the germylene [Ge(dtb-bian)] has a *syn* orientation of the 2,5-disubstituted phenyl rings.[4e] The NMR

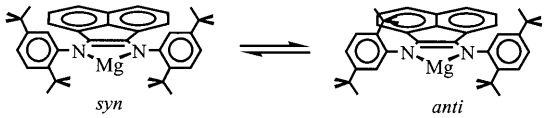

Figure 2. Interconversion of *syn* and *anti* isomers in Mg–dtb-bian complexes.

spectroscopic data for [Mg(dtb-bian)(thf)$_2$][4c] and [Ge(dtb-bian)][4e] indicate that in solution interconversion of *syn* and *anti* isomers takes place.

Before we discuss of the solution behavior of **6** it is worth noting that in all the magnesium complexes which contain the protonated amido/amino dpp-bian ligand, the anionic ligands formed upon deprotonation (e.g. phenylethynyl or enolate) are placed in the pocket formed between two *i*Pr groups of two phenyl rings. Furthermore, these anionic ligands and the hydrogen attached to N atom are always positioned on the same side of the metallocycle. Besides, the *i*Pr substituents are orientated in such a way that the four methine protons of *i*Pr groups are directed towards metallocycle, whereas the methyl groups are directed away from the metal. Apparently, this minimizes the overcrowding of the metal coordination sphere. A placement of the ketenimine ligand between two *ortho-tert*-butyl substituents in the molecule of **6** with *syn* orientation seemed impossible due to the steric reasons. However, if a molecule of **6** with *syn* orientation the keteniminate ligand is positioned between *meta-tert*-butyl substituents and the amino proton is delocalized between two nitrogen atoms, only two ^{1}H signals of the *t*Bu

groups should be expected. The ^{1}H NMR spectrum of **6** in [D$_8$]THF reveals four signals of *t*Bu substituents centered at $\delta = 1.49$ (9H), 1.34 (9H), 1.11 (9H) and 1.06 (9H) ppm correspondingly. Based on these data one may conclude that in solution the molecules of **6** have an *anti* orientation of the phenyl rings with the proton being attached to one nitrogen atom. The signal of the amino proton is shifted high field relative to that in **5** and appears at $\delta = 5.74$ ppm. Very similar chemical shifts have been observed for the amino proton in (dtb-bian)H$_2$ in [D$_8$]THF (5.77 ppm).[2c]

Molecular structures of 2, 3, 7, and 8: The molecular structures of **2**, **3**, **7** and **8** are depicted in Figures 3–6 respectively. The crystallographic data obtained for **3** are of insufficient quality for the thorough discussion. Therefore, Figure 4 depicts only the atom connectivity in **3**. The crystal data collection and structure refinement data for **2**, **7** and **8** are listed in Table 1, selected bond lengths and angles in Tables 2 and 3, respectively.

The molecular structure of **2** can be compared with that of closely related calcium complex [Ca(dpp-bian)(thf)$_4$].[1] The strontium atom in **2** is six-coordinate and has a distorted octahedral environment (Figure 3). Due to the larger ionic radius of Sr^{2+} relative to Ca^{2+}, all the metal–ligand distances in **2** are elongated by approximately 0.13 Å. As in the calcium complex one of the four metal–oxygen bonds in **2** is significantly longer (Sr–O(1) 2.673 Å) than the other three, which are in a range of 2.537–2.578 Å. The shortest Sr–O(3) distance is observed for the THF molecule that fits into the pocket formed by two isopropyl groups. The angle between the plane formed with N(1)-N(2)-Sr and the donor atom O(3) is 101.4°. In contrast to the Mg–N bonds in **1** (2.105 and 2.045 Å), the two Sr–N bonds (2.505 and 2.497 Å) are almost of the same length, and, as expected, they are approximately 0.1 Å longer than those found in the calcium complex (Ca–N, 2.396 and 2.382 Å).[1] Owing the longer Sr–N distances, the bite angle N(1)-Sr-N(2) (72.4°) in **2** is somewhat smaller than the angle N(1)-Ca-N(2) (75.8°) in [Ca(dpp-bian)(thf)$_4$].[1]

In the solid state, the molecule of **3** is a dimer formed from two DME-bridged {Ba(dpp-bian)(dme)$_2$} fragments (Figure 4). The barium atoms in **3** are seven-coordinate.

The barium atom in the molecule of **7** is seven-coordinate (Figure 5). The significant differences in the length of the

Table 2. Selected bond lengths [Å] for **2**, **7** and **8**.

	2	**7**	**8**
M–N(1)	2.505(2)	2.6989(16)	2.501(2)
M–N(2)	2.497(2)	3.0062(17)	2.677(2)
M–N(3)		2.7385(18)	2.559(3)
M–N(4)			2.822(2)
M–N(4A)			2.608(2)
M–O(1)	2.6731(19)	2.8308(14)	2.493(2)
M–O(2)	2.5599(19)	2.7619(14)	
M–O(3)	2.5368(18)	2.7465(14)	
M–O(4)	2.5776(18)	2.8337(14)	
N(1)–C(1)	1.397(3)	1.339(2)	1.348(3)
N(1)–C(13)	1.416(3)	1.414(2)	1.422(3)
N(2)–H(2)		0.7933	0.95(2)
N(2)–C(2)	1.387(3)	1.442(3)	1.419(3)
N(2)–C(25)	1.409(3)	1.414(2)	1.433(3)
N(3)–C(37)		1.170(3)	
N(3)–C(41)			1.306(4)
C(1)–C(2)	1.394(4)	1.398(3)	1.395(4)
C(37)–C(38)		1.386(3)	
C(38)–C(39)		1.452(3)	
C(38)–C(45)		1.478(3)	
C(41)–C(44)			1.505(4)
C(41)–C(42)			1.403(4)
C(42)–C(43)			1.381(5)
C(43)–N(4)			1.160(4)

Table 1. Crystal data and structure refinement details for **2**, **7** and **8**.

	2	**7**	**8**
formula	$C_{54}H_{76}SrN_2O_{4.50}$	$C_{70}H_{83}BaN_3O_4$	$C_{100}H_{120}Sr_2N_8O_2$
M_r	912.79	1167.73	1641.28
T [K]	100(2)	100(2)	120(2)
λ [Å]	0.71073	0.71073	0.71073
crystal system	monoclinic	monoclinic	monoclinic
space group	$P2_1/n$	$P2_1/c$	$P2_1/n$
a [Å]	13.4224(8)	15.7865(8)	12.7225(6)
b [Å]	18.6715(11)	22.9528(11)	19.4015(9)
c [Å]	19.5886(12)	17.3644(8)	18.3391(8)
β [°]	98.7690(10)	104.9960(10)	94.2980(10)
V [Å^3]	4851.8(5)	6077.6(5)	4514.0(4)
Z	4	4	2
ρ_{calcd} [g cm^{-3}]	1.250	1.276	1.208
μ [mm^{-1}]	1.159	0.704	1.234
F(000)	1952	2448	1736
crystal size [mm^3]	$0.10\times0.08\times0.03$	$0.24\times0.20\times0.19$	$0.50\times0.31\times0.23$
$\theta_{min}/\theta_{max}$	1.52/23.00	1.77/25.00	1.53/25.00
index ranges	$-14\le h\le 14$	$-18\le h\le 18$	$-15\le h\le 11$
	$-20\le k\le 20$	$-27\le k\le 17$	$-23\le k\le 23$
	$-21\le l\le 19$	$-20\le l\le 20$	$-21\le l\le 19$
reflections collected	21840	34472	24775
independent reflections	6755	10705	7944
R_{int}	0.0452	0.0255	0.0379
completeness to θ_{max} [%]	99.9	99.9	99.9
max/min transmission	0.9661/0.8929	0.8779/0.8492	0.7645/0.5774
data/restraints/parameters	6755/2/847	10705/0/1035	7944/0/541
GOF on F^2	1.009	1.032	1.056
final R indices [$I>2\sigma(I)$]	$R_1=0.0340$	$R_1=0.0263$	$R_1=0.0436$
	$wR_2=0.0750$	$wR_2=0.0634$	$wR_2=0.1066$
R indices (all data)	$R_1=0.0548$	$R_1=0.0343$	$R_1=0.0680$
	$wR_2=0.0802$	$wR_2=0.0658$	$wR_2=0.1135$
largest diff. peak/hole [e Å^{-3}]	0.521/−0.275	0.674/−0.231	0.926/−0.446

Table 3. Selected bond angles [°] for **2**, **7**, and **8**.

	2	**7**	**8**
N(1)-M-N(2)	72.36(7)	62.13(5)	68.20(7)
N(1)-M-O(1)	162.55(6)	130.48(5)	95.74(7)
N(1)-M-O(2)	92.95(7)	92.03(5)	
N(1)-M-O(3)	90.17(7)	114.97(5)	
N(1)-M-O(4)	117.22(7)	143.15(5)	
N(2)-M-O(1)	114.31(7)	157.57(5)	154.93(7)
N(2)-M-O(2)	156.41(7)	143.94(5)	
N(2)-M-O(3)	110.25(6)	90.69(4)	
N(2)-M-O(4)	90.89(6)	81.08(5)	
O(1)-M-O(2)	85.21(6)	58.49(4)	
O(1)-M-O(3)	72.43(6)	97.51(4)	
O(1)-M-O(4)	79.55(6)	84.97(4)	
O(2)-M-O(3)	87.57(6)	77.40(4)	
O(2)-M-O(4)	79.34(6)	119.37(4)	
O(3)-M-O(4)	149.94(6)	60.16(4)	
C(1)-N(1)-M	108.68(16)	119.26(12)	116.03(16)
C(13)-N(1)-M	132.17(16)	120.46(16)	124.61(15)
C(2)-N(2)-M	109.12(16)	107.69(11)	108.64(15)
C(25)-N(2)-M	132.76(16)	122.09(12)	122.49(17)
N(3)-C(37)-C(38)		177.4(2)	
C(37)-C(38)-C(39)		119.32(19)	
C(37)-N(3)-M		147.56(16)	
N(3)-M-N(4)			77.47(8)
N(4A)-M-N(4)			74.79(9)
M(A)-N(4)-M			105.21(9)
N(3)-C(41)-C(44)			121.7(3)
C(42)-C(41)-C(44)			117.8(3)
C(43)-C(42)-C(41)			118.5(3)

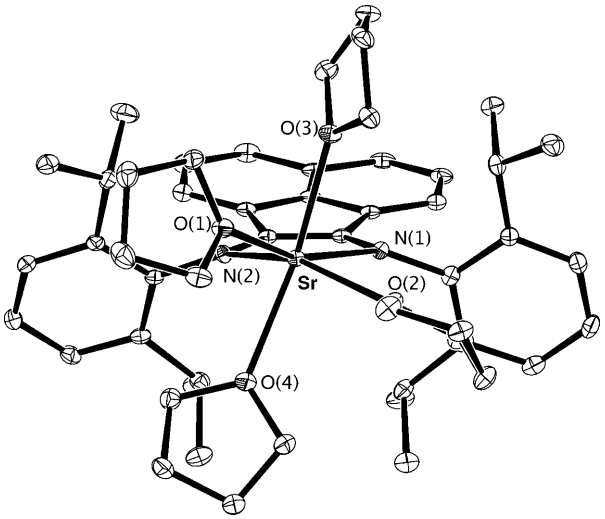

Figure 3. ORTEP drawing of complex **2** with thermal ellipsoids drawn at 30% probability level. Hydrogen atoms are omitted for clarity.

Ba–N(dpp-bian) bonds (Ba–N(1) 2.699 Å; Ba–N(2) 3.006 Å) reflect the different strength of the metal coordination of the amido (N(1)) and the amino (N(2)) functions. This difference (ca. 0.31 Å) corresponds well with that found for the product obtained by addition of phenylacetylene to **1** [Mg(dpp-bianH)(C≡CPh)(thf)$_2$] (2.355 and 2.045 Å)[2b] as well as with those in the magnesium enolates [Mg(dpp-bianH){OC(=CHPh)CH$_2$Ph}(thf)$_2$] (Mg–N: 2.066 and 2.369 Å), [Mg(dpp-bianH){OC(=CPh$_2$)CH$_3$}(thf)$_2$] (Mg–

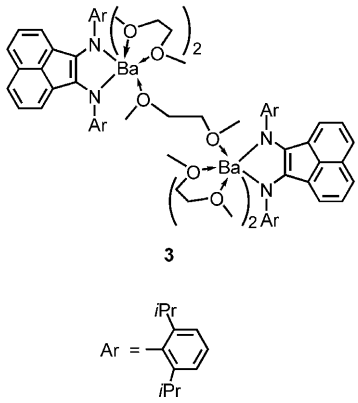

Figure 4. Atom connectivity in **3** determined by single-crystal X-ray diffraction.

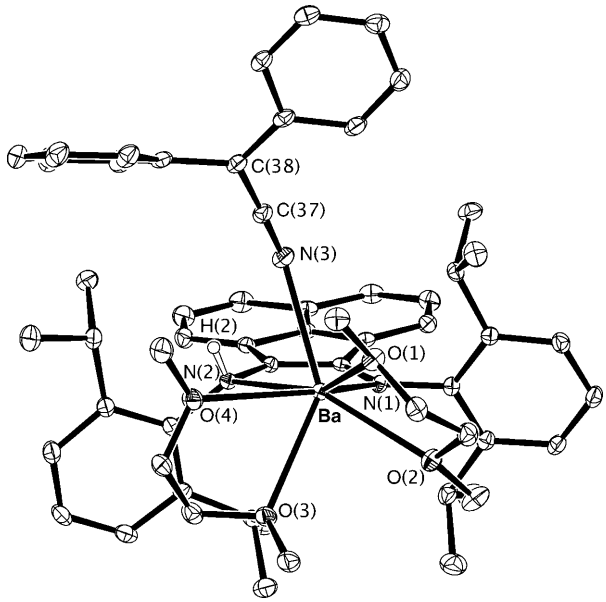

Figure 5. ORTEP drawing of complex **7** with thermal ellipsoids drawn at 30% probability level. Hydrogen atoms with exception of H(2) are omitted for clarity.

N: 2.051 and 2.410 Å), but is less than that in [Mg(dpp-bianH)(camphor)(py)$_2$] (Mg–N: 2.055 and 2.436 Å), which formed under addition of enolisable ketones to **1**.[2d] In **7** each of two bidentate DME molecules has one short and one long Ba–O distance (Ba–O(1) 2.830, Ba–O(2) 2.762 and Ba–O(3) 2.746, Ba–O(4) 2.834 Å). The shortening of Ba–O(3) distance can be explained by the short intermolecular C(57)···N(3) interatction (3.134(3) Å, which is less of sum of Van-der-Waals radii, 3.20 Å) between neighboring molecules. This difference in the Ba–O(1) and Ba–O(2) distances is not truly understood, but apparently may be explained so by an influence of the steric factors. In **7** the keteniminate ligand and the amine hydrogen H(2) are placed on the same side of the plane formed by the metallocycle Ba-N(1)-C(1)-C(2)-N(2). The torsion angle H(2)-N(2)-Ba-N(3)

(17.7°) is somewhat larger than those in the three above-mentioned enolates (7.0°, 17.2°, and 8.1°, respectively).

To date there are only few examples of crystallographically characterized metal–keteniminate complexes.[13] The lithium and indium derivatives, $[\{Li(\mu\text{-}Ph_2CCN)(Et_2O)_2\}_2]$[13a] and $[\{In(\mu\text{-}Ph_2CCN)Me_2(thf)\}_2]$[13a] have the same keteniminate ligand as in **7**. Whereas the keteniminate group in the Li and In complexes acts as μ_2-bridging ligand the $Ph_2C{=}C{=}N$ group in **7** is a terminal one. It is worth noting that in the phenylethynyl derivative $[\{Mg(dpp\text{-}bianH)\}(C{\equiv}CPh)(thf)_2]$[2b] and in enolates $[Mg(dpp\text{-}bianH)\{OC(=CHPh)CH_2Ph\}(thf)_2]$, $[Mg(dpp\text{-}bianH)\{OC(=CPh_2)CH_3\}(thf)_2]$, and $[Mg(dpp\text{-}bianH)(camphor)(py)_2]$[2d] the $PhC{\equiv}C$- and $R_2C{=}C(R)O$ groups are terminal as well. Evidently, this general feature is caused by the rigidity and bulkiness of dpp-bian ligand, which prevents the formation of dimers through bridging ligands. The Ba–N(3) bond is 2.738 Å, which is predictably much longer than the M–N distances in $[\{Li(\mu\text{-}Ph_2C{=}C{=}N)(Et_2O)_2\}_2]$ (2.25 and 2.46 Å) and $[\{In(\mu\text{-}Ph_2C{=}C{=}N)Me_2(thf)\}_2]$ (2.03 and 2.06 Å).[13a] The heteroallen type of the keteniminate ligand in **7** is demonstrated by the shortening of the C(37)–C(38) bond (1.386 Å) and elongation of the C(37)–N(3) bond (1.170 Å) relative to those bonds in free $Ph_2HC\text{-}C{\equiv}N$ (1.470 and 1.147 Å, respectively).[13a] Similar bond allocation is observed in Li and In complexes cited above. The core C(38)-C(37)-N(3) in **7** is almost linear (177.4°).

The dimeric structure of **8** has a crystallographically imposed inversion center with two {Sr(dpp-bianH)(thf)} moieties connected by two crotonitrileamido ligands (Figure 6). Each strontium atom in **8** displays distorted octahedral geometry formed by the chelating amido/amino dpp-bian ligand, one THF molecule, and the tridentate crotonitrileamido ligand.

As in **7** the amido and amino functions of the dpp-bian ligand in **8** are clearly visible from the difference in Sr–N(dpp-bian) distances (Sr–N(1) 2.501, Sr–N(2) 2.677 Å). According to the hypothesis that the addition of the first equivalent of $CH_3C{\equiv}N$ to complex **2** proceeds via formation of the intermediate ketenimido complex the proton H(2) turns to be with N(3) at the same plane of the chealting system. The amido N(3) atom originates from the transitional ketenimido ligand, which after insertion of second equivalent of $CH_3C{\equiv}N$ rearranges through a 1,3-H shift to crotonitrileamido ligand. The geometry of the crotonitrileamido ligands in **8** can be compared with that in rhenium, lithium, and yttrium complexes, $[\{Re(bpy)(CO)_3\}_2\{N(H)C(CH_3)C(H)CN\}]$,[11] $[\{LiPy_2[N(H)C(CH_3)C(H)CN]\}_2]$[9] $[\{Y[Me_2Si(NCMe_3)OCMe_3)]_2[N(H)C(CH_3)C(H)CN]\text{-}(thf)\}_2]$.[10] These three complexes are the only examples of crystallographically characterized compounds that consist of bridging crotonitrileamido ligand. As for the lithium and yttrium complexes, in compound **8** two crotonitrileamido ligands connect two metal atoms. In lithium and yttrium complexes this results in the formation of the 12-membered metallocycle. In contrast, in the molecule of **8** the crotonitrileamido ligands are arranged in such a way that nitrile atoms N(4) and N(4A) bound to both Sr atoms, thus dividing the 12-membered metallocycle into three cycles. The difference in the arrangement of crotonitrileamido ligands in Li and Y complexes with respect to complex **8** is that in case of **8** the metal atom bound to N(3) is in the *trans* position to the CH_3 group of the ligand, whereas in the Li and Y complexes the metals are in the *cis* position. In complex $[\{Re(bpy)(CO)_3\}_2\{N(H)C(CH_3)C(H)CN\}]$[11] one Re atom is connected to the amido function in the way similar to that in **8**.

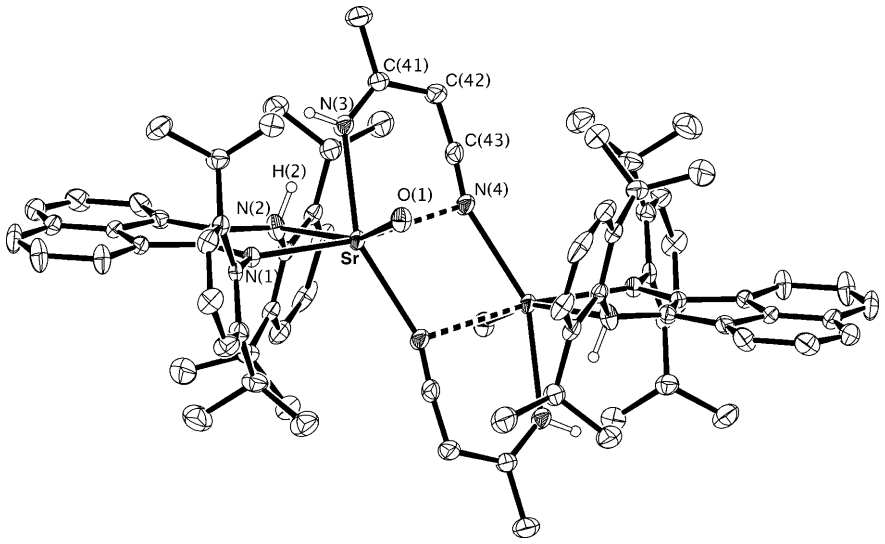

Figure 6. ORTEP drawing of complex **8** with thermal ellipsoids drawn at 30% probability level. Hydrogen atoms with exception of H(2) and the THF carbon atoms are omitted for clarity.

Conclusion

We could demonstrate that the alkaline earth metal complexes of the rigid dianionic acenaphthenediimine ligands can deprotonate nitriles to give keteniminate species. In contrast to the reactions of alkali-metal reagents, magnesium amides or yttriumalkyls with nitriles, which run with amine or alkane elimination the above reactions proceed by addition of the nitriles with formation of Mg, Sr, and Ba keteniminates and simultaneous protonation of one nitrogen atom of the bian ligand.

Experimental Section

General remarks: All manipulations were carried out under vacuum using Schlenk ampoules. The solvents THF, DME, benzene, and toluene were

dried by distillation from sodium benzophenone. The deuterated solvents [D$_8$]THF and C$_6$D$_6$ used for the NMR measurements were dried with sodium benzophenone at ambient temperature, and just prior to use, condensed under vacuum into the NMR tubes already containing the respective compounds. Melting points were measured in sealed capillaries. The IR spectra were recorded on a Specord M80 spectrometer, the ^{1}H NMR spectra were obtained on a Bruker DPX-200 NMR spectrometer.

[Sr(dpp-bian)(thf)$_4$] (2): Strontium pieces (4.4 g, 50 mmol) and I$_2$ (0.4 g, 1.6 mmol) were placed in a Schlenk-like ampoule (ca. 100 mL volume) equipped with a Teflon stopcock. After evacuation of the ampoule (at 10^{-1} Torr for ca. 1 min), THF (40 mL) was added by condensation and the mixture was stirred for 2 h. After the mixture decolorized the formed [SrI$_2$(thf)$_n$] was decanted together with the solvent and the residual metal was washed three times with THF (40 mL). A suspension of dpp-bian (0.5 g, 1.0 mmol) in THF (40 mL) was then added to the activated strontium metal and the mixture was refluxed for 30 min. In the course of the reaction, the mixture turned first deep red and then deep brown. The solution was then cooled to ambient temperature and decanted from the excess of strontium. Evaporation of solvent from mother liquor gave 0.88 g (97%) of compound **2** as a deep red crystalline solid. Crystallization of the crude product from THF (10 mL) yielded 0.48 g of **2**·0.5(C$_4$H$_8$O) as large block-like crystals suitable for X-ray crystal structure analysis. M.p. >220°C (decomp); elemental analysis calcd (%) for C$_{52}$H$_{72}$SrN$_2$O$_4$·0.5(C$_4$H$_8$O) (912.79): C 71.05, H 8.39; found: C 70.91, H 8.29; ^{1}H NMR (200 MHz, [D$_8$]THF, 20°C): δ = 7.6–6.1 (m, 12H; C-H$_{arom}$), 4.06 (sept, 4H; C*H*Me$_2$), 3.54 (s, 16H; α-C*H*$_2$-THF), 1.73 (s, 16H; β-C*H*$_2$-THF), 1.52 (d, J = 6.8 Hz, 12H; CH(C*H*$_3$)$_2$), 1.43 ppm (d, J = 6.8 Hz, 12H; CH(C*H*$_3$)$_2$); IR (Nujol): $\tilde{\nu}$ = 1575 (s), 1405 (m), 1395 (w), 1375 (m), 1340 (w), 1300 (s), 1230 (m), 1200 (w), 1165 (s), 1090 (w), 1075 (s), 1020 (vs), 995 (w), 955 (w), 925 (w), 905 (vs), 895 (s), 870 (s), 840 (s), 785 (m), 745 (s), 715 (m), 665 (m), 610 (m), 595 (m), 530 (m), 500 cm^{-1} (m).

[Ba(dpp-bian)(dme)$_{2.5}$] (3): Barium pieces (3.5 g, 25.5 mmol) and I$_2$ (0.3 g, 1.2 mmol) were placed in a Schlenk-like ampoule (ca. 100 mL volume) equipped with a Teflon stopcock. After evacuation of the ampoule (at 10^{-1} Torr for ca. 1 min), DME (30 mL) was added by condensation and the mixture was stirred for 4 h. After the mixture decolorized the formed [BaI$_2$(thf)$_n$] was decanted together with the solvent and the residual metal was washed two times with DME (30 mL). A suspension of dpp-bian (0.5 g, 1.0 mmol) in DME (30 mL) was then added to the activated barium metal and the mixture was heated for 60 min at 80°C. In the course of the reaction, the mixture turned first deep red and then deep brown. The solution was then cooled to ambient temperature and filtered off. Evaporation of the solvent from mother liquor afforded 0.84 g (98%) of compound **3** as deep red crystalline solid. M.p. >200°C (decomp); elemental analysis calcd (%) for C$_{92}$H$_{130}$Ba$_2$N$_4$O$_{10}$ (1726.73): C 63.99, H 7.59; found: C 63.70, H 7.37. The signals in ^{1}H NMR spectra of **3** in [D$_8$]THF and C$_6$D$_6$ were very broad. In the ^{1}H NMR spectrum in [D$_8$]THF the signals associated with CH$_3$ groups of the *i*Pr substituents appear as broad singlet at δ = 1.12 ppm (24H). An accurate assignment of other signals was difficult. IR (Nujol): $\tilde{\nu}$ = 1590 (s), 1405 (m), 1345 (m), 1285 (m), 1240 (m), 1195 (w), 1150 (m), 1100 (m), 1050 (s), 980 (w), 945 (w), 900 (m), 875 (w), 830 (s), 800 (w), 790 (m), 755 (vs), 725 (w), 700 (w), 665 (w), 600 (m), 585 cm^{-1} (w).

[Mg(dpp-bianH)(NCCPh$_2$)(thf)$_2$] (5): Ph$_2$HCCN (0.19 g, 1 mmol) was added to a solution of **1** (in situ from 0.5 g (1 mmol) of dpp-bian) in THF (40 mL) diphenylacetonitrile. The reaction mixture turned blue-green. The solvent was removed in vacuum and the residue dissolved in benzene (40 mL). The deep blue solution formed was then concentrated to 20 mL by evaporation of the solvent in vacuum. After two days plate-like crystals of **5** were collected by decantation of solution and drying of the solid in vacuum. Yield 0.37 g (43%); m.p. 172°C (decomp); elemental analysis calcd (%) for C$_{58}$H$_{67}$MgN$_3$O$_2$ (862.48): C 80.77, H 7.83; found: C 80.63, H 7.47; ^{1}H NMR (200 MHz, [D$_8$]THF, 20°C): δ = 7.32 (d, J = 8.0 Hz, 1H; C-H$_{arom}$), 7.17–7.07 (m, 10H; C-H$_{arom}$), 6.90–6.70 (m, 7H; C-H$_{arom}$), 6.47 (t, J = 7.3 Hz, 2H; C-H$_{arom}$), 6.06 (s, 1H; N-H), 5.98 (d, J = 7.0 Hz, 1H; C-H$_{arom}$), 5.81 (d, J = 6.5 Hz, 1H; C-H$_{arom}$), 3.73 (sept, J = 6.8 Hz, 2H; C*H*Me$_2$), 3.57 (m, 8H; α-C*H*$_2$-THF), 3.44 (sept, J = 6.8 Hz, 2H; C*H*Me$_2$), 1.73 (m, 8H; β-C*H*$_2$-THF), 1.18 (d, J = 6.8 Hz, 6H; CH(C*H*$_3$)$_2$), 1.16 (d, J = 6.8 Hz, 6H; CH(C*H*$_3$)$_2$), 0.89 ppm (d, J = 6.8 Hz, 12H; CH(C*H*$_3$)$_2$); IR (Nujol): $\tilde{\nu}$ = 3296 (w), 2086 (vs), 1590 (s), 1515 (s), 1300 (m), 1285 (m), 1150 (m), 1000 (w), 865 (m), 790 (s), 755 (vs), 700 (vs), 665 (w), 600 (w), 505 (s), 470 (m), 455 (m), 430 cm^{-1} (s).

[Mg(dtb-bianH)(NCCPh$_2$)(thf)$_2$] (6): Ph$_2$HCCN (0.19 g, 1 mmol) was added to a solution of **4** (in situ from 0.56 g (1 mmol) of dtb-bian) in THF (40 mL). The solvent was removed in vacuum and the residue dissolved in toluene (40 mL). Toluene was evaporated and the remaining solid was dissolved in Et$_2$O (200 mL). On concentration of this solution in vacuum to a volume of about 15 mL, the product **6**·Et$_2$O precipitated as deep blue crystals. Yield 0.62 g (63%); m.p. 105°C (decomp); elemental analysis calcd (%) for C$_{66}$H$_{85}$MgN$_3$O$_3$·Et$_2$O (992.70): C 79.85, H 8.63; found: C 79.10, H 8.21; ^{1}H NMR (200 MHz, [D$_8$]THF, 20°C): δ = 7.46 (d, J = 8.3 Hz, 1H; C-H$_{arom}$), 7.22–6.46 (m, 20H; C-H$_{arom}$), 5.83 (br s, 1H; C-H$_{arom}$), 5.74 (s, 1H; N-H), 3.58 (m, 8H; α-C*H*$_2$-THF), 3.35 (quart, J = 7.0 Hz, 4H; Et$_2$O), 1.73 (m, 8H; β-C*H*$_2$-THF), 1.49 (s, 9H; C(C*H*$_3$)$_3$), 1.34 (s, 9H; C(C*H*$_3$)$_3$), 1.11 (s, 9H; C(C*H*$_3$)$_3$), 1.08 (t, 6H; J = 7.0 Hz, Et$_2$O), 1.06 ppm (s, 9H; C(C*H*$_3$)$_3$); IR (Nujol): $\tilde{\nu}$ = 3346 (w), 2088 (vs), 1590 (s), 1515 (s), 1450 (s), 1380 (s), 1265 (m), 1200 (w), 1110 (m), 1075 (m), 1020 (s), 1000 (w), 970 (w), 920 (m), 865 (s), 810 (m), 750 (s), 690 (s), 530 (w), 500 (s), 470 cm^{-1} (s).

[Ba(dpp-bianH)(NCCPh$_2$)(dme)$_2$] (7): A solution of Ph$_2$HCCN (0.19 g, 1 mmol) in DME (10 mL) was added to a cooled (−15°C) solution of **3** in DME (40 mL), prepared as described above. The reaction mixture was warmed up and stored at ambient temperature for 30 min. After heating of the dark mixture for 5 min at 50°C with partial evaporation of the solvent under vacuum, the solution turned deep blue. The solvent was removed in vacuum and the residue dissolved in benzene (40 mL). The deep blue solution was then concentrated to 20 mL by evaporation of the solvent in vacuum. After 3 days deep blue prismatic crystals of **7**·2C$_6$H$_6$ were isolated in 53% (0.61 g) yield. M.p. 146°C (decomp); elemental analysis calcd (%) for C$_{58}$H$_{71}$BaN$_3$O$_4$·2C$_6$H$_6$ (1167.75): C 72.00, H 7.16; found: C 72.01, H 7.12; ^{1}H NMR (200 MHz, [D$_8$]THF, 20°C): δ = 7.32 (d, J = 8.0 Hz, 8H; C-H$_{arom}$), 7.17–7.07 (m, 10H; C-H$_{arom}$), 6.90–6.70 (m, 7H; C-H$_{arom}$), 6.47 (t, J = 7.3 Hz, 2H; C-H$_{arom}$), 6.06 (t, 1H; N-H), 5.98 (d, J = 7.0 Hz, 1H; C-H$_{arom}$), 5.81 (d, J = 6.5 Hz, 1H; C-H$_{arom}$), 3.73 (sept, J = 6.8 Hz, 2H; C*H*Me$_2$), 3.57 (m, 8H; α-C*H*$_2$-THF), 3.44 (sept, J = 6.8 Hz, 2H; C*H*Me$_2$), 1.73 (m, 8H; β-C*H*$_2$-THF), 1.18 (d, J = 6.8 Hz, 6H; CH(C*H*$_3$)$_2$), 1.16 (d, J = 6.8 Hz, 6H; CH(C*H*$_3$)$_2$), 0.89 ppm (d, J = 6.8 Hz, 12H; CH(C*H*$_3$)$_2$); IR (Nujol): $\tilde{\nu}$ = 2075 (vs), 1570 (vs), 1500 (w), 1300 (w), 1285 (w), 1230 (s), 1170 (s), 1100 (s), 1040 (s), 1015 (w), 970 (m), 905 (m), 835 (m), 795 (m), 740 (vs), 685 (s), 505 cm^{-1} (m).

[{Sr(dpp-bianH)[N(H)C(CH$_3$)C(H)CN](thf)}$_2$] (8): Acetonitrile (82 mg, 2 mmol) was added by condensation in vacuum at −30°C to solution of **2** in THF (40 mL), prepared as described above. Warming the reaction mixture up to ambient temperature caused color change from brown to deep blue. The solvent was removed in vacuum and the residue dissolved in benzene (40 mL). The deep blue solution was then concentrated to 20 mL by evaporation of the solvent in vacuum. After two days block-like deep blue crystals of **8** were collected by decantation of the solution and drying of the solid in vacuum at ambient temperature. Yield 0.43 g (52%); mp. >180°C (decomp); elemental analysis calcd (%) for C$_{88}$H$_{108}$SrN$_8$O$_2$·2C$_6$H$_6$ (1641.28): C 73.18, H 7.37; found: C 73.23, H 7.42. The ^{1}H NMR spectra of **8** in [D$_8$]THF, C$_6$D$_6$ and [D$_5$]pyridine were uninformative due to the extreme broadening of all signals. For example, the ^{1}H NMR spectrum in [D$_5$]pyridine revealed no separated resonances in the aromatic region, except for the signal of the residual protons of [D$_5$]pyridine and benzene, which is present in the lattice of compound **8**. The CH and CH$_3$ signals of the *i*Pr substituents of the phenyl rings appeared as broad singlets at δ = 3.83 ppm (4H) and 1.12 (24H), respectively. The methyl signal of the crotonitrileamido ligand was positioned at δ = 1.66 ppm (3H). IR (Nujol): $\tilde{\nu}$ = 3295 (w), 2080 (vs), 1575 (s), 1515 (s), 1495 (s), 1465 (s), 1410 (s), 1370 (vs), 1340 (w), 1300 (w), 1275 (m), 1235 (m), 1210 (w), 1180 (s), 1140 (m), 1090 (m), 1060 (w), 1015 (s), 1000 (w), 975 (m), 910 (s), 870 (s), 820 (m), 795 (s), 765 (vs), 700 (w), 665 (s), 600 (m), 520 cm^{-1} (m).

Single-crystal X-ray structure determinations of 2, 7, and 8: The crystal data and details of data collection are given in Table 1. The data were

collected on a Bruker SMART APEX diffractometer (graphite-monochromated $Mo_{K\alpha}$ radiation, ω- and ϕ-scan technique, $\lambda = 0.71073$ Å) at 100 K. The structures were solved by direct methods by using SHELXS-97[14] and were refined on F^2 by using SHELXL-97.[15] All non-hydrogen atoms were refined anisotropically. The hydrogen atoms in **2** (except the H atoms in solvate C_4H_8O molecule) and **7** were found from the Fourier synthesis and refined isotropically. The hydrogen atoms of lattice benzene molecule as well as H(2), H(3), and H(42) were found from Fourier synthesis and refined isotropically, whereas all other H atoms in **8** were placed in calculated positions and refined in the "riding-model". SADABS[16] was used to perform area-detector scaling and absorption corrections. The geometrical aspects of the structures were analyzed by using the PLATON program.[17] CCDC-265971 (**2**), CCDC-265972 (**7**), CCDC-265973 (**8**) contain the supplementary crystallographic data for this paper. These data can be obtained free of charge from The Cambridge Crystallographic Data Centre via www.ccdc.cam.ac.uk/data_request/cif.

Acknowledgements

This work was supported by the Russian Foundation for Basic Research (Grant No. 03–03–32246) and the Russian Science Support Foundation (ILF).

[1] I. L. Fedushkin, A. A. Skatova, V. A. Chudakova, G. K. Fukin, S. Dechert, H. Schumann, *Eur. J. Inorg. Chem.* **2003**, 3336–3346.

[2] a) I. L. Fedushkin, A. A. Skatova, V. K. Cherkasov, V. A. Chudakova, S. Dechert, M. Hummert, H. Schumann, *Chem. Eur. J.* **2003**, *9*, 5778–5783; b) I. L. Fedushkin, N. M. Khvoinova, A. A. Skatova, G. K. Fukin, *Angew. Chem.* **2003**, *115*, 5381–5384; *Angew. Chem. Int. Ed.* **2003**, *42*, 5223–5226; c) I. L. Fedushkin, V. A. Chudakova, G. K. Fukin, S. Dechert, M. Hummert, H. Schumann, *Russ. Chem. Bull.* **2004**, *53*, 2744–2750; d) I. L. Fedushkin, A. A. Skatova, G. K. Fukin, M. Hummert, H. Schumann, *Eur. J. Inorg. Chem.* **2005**, 2332–2338; e) I. L. Fedushkin, A. A. Skatova, A. N. Lukoyanov, V. A. Chudakova, S. Dechert, M. Hummert, H. Schumann, *Russ. Chem. Bull.* **2004**, *53*, 2751–2762; f) V. M. Makarov, G. K. Fukin, I. L. Fedushkin, unpublished results; g) I. L. Fedushkin, V. A. Chudakova, G. K. Fukin, unpublished results.

[3] a) M. W. van Laren, C. J. Elsevier, *Angew. Chem.* **1999**, *111*, 3926–3929; *Angew. Chem. Int. Ed.* **1999**, *38*, 3715–3717; b) R. van Belzen, H. Hoffmann, C. J. Elsevier, *Angew. Chem.* **1997**, *109*, 1833–1835; *Angew. Chem. Int. Ed. Engl.* **1997**, *36*, 1743–1745; c) G. A. Grasa, R. Singh, E. D. Stevens, S. P. Nolan, *J. Organomet. Chem.* **2003**, *687*, 269–279; d) A. Heumann, L. Giordano, A. Tenaglia, *Tetrahedron Lett.* **2003**, *44*, 1515–1518; e) A. E. Cherian, E. B. Lobkovsky, G. W. Coates, *Chem. Commun.* **2003**, 2566–2567; f) M. D. Leatherman, S. A. Svejda, L. K. Johnson, M. Brookhart, *J. Am. Chem. Soc.* **2003**, *125*, 3068–3081; g) J. Kiesewetter, W. Kaminsky, *Chem. Eur. J.* **2003**, *9*, 1750–1758.

[4] a) I. L. Fedushkin, A. A. Skatova, V. A. Chudakova, G. K. Fukin, *Angew. Chem.* **2003**, *115*, 3416–3420; *Angew. Chem. Int. Ed.* **2003**, *42*, 3294–3298; b) I. L. Fedushkin, A. A. Skatova, V. A. Chudakova, V. K. Cherkasov, G. K. Fukin, M. A. Lopatin, *Eur. J. Inorg. Chem.* **2004**, 388–393; c) I. L. Fedushkin, V. A. Chudakova, A. A. Skatova, N. M. Khvoinova, Yu. A. Kurskii, T. A. Glukhova, G. K. Fukin, S. Dechert, M. Hummert, H. Schumann, *Z. Anorg. Allg. Chem.* **2004**, *630*, 501–507; d) I. L. Fedushkin, N. M. Khvoinova, A. Yu. Baurin, G. K. Fukin, V. K. Cherkasov, M. P. Bubnov, *Inorg. Chem.* **2004**, *43*, 7807–7815; e) I. L. Fedushkin, A. A. Skatova, V. A. Chudakova, N. M. Khvoinova, A. Yu. Baurin, S. Dechert, M. Hummert, H. Schumann, *Organometallics* **2004**, *23*, 3714–3718; f) I. L. Fedushkin, A. A. Skatova, V. A. Chudakova, V. K. Cherkasov, S. Dechert, H. Schumann, *Russ. Chem. Bull.* **2004**, *53*, 2142–2147; g) H. Schumann, M. Hummert, A. N. Lukoyanov, I. L. Fedushkin, *Organometallics* **2005** in press.

[5] I. L. Fedushkin, A. A. Skatova, M. Hummert, H. Schumann, *Eur. J. Inorg. Chem.* **2005**, 1601–1608.

[6] a) J. F. Allan, W. Clegg, K. W. Henderson, L. Horsburgh, A. R. Kennedy, *J. Organomet. Chem.* **1998**, *559*, 173–179; b) J. F. Allan, K. W. Henderson, A. R. Kennedy, *Chem. Commun.* **1999**, 1325–1326; c) J. F. Allan, K. W. Henderson, A. R. Kennedy, S. J. Teat, *Chem. Commun.* **2000**, 1059–1060.

[7] K. C. Yang, C. C. Chang, J. Y. Huang, C. C. Lin, G. H. Lee, Y. Wang, M. Y. Chiang, *J. Organomet. Chem.* **2002**, *648*, 176–187.

[8] G. A. Reynolds, W. J. Humphlett, F. W. Swamer, C. R. Hauser, *J. Org. Chem.* **1951**, *16*, 165–172.

[9] A. G. Avent, A. D. Frankland, P. B. Hitchcock, M. F. Lappert, *Chem. Commun.* **1996**, *21*, 2433–2434.

[10] R. Duchateau, T. Tuinstra, E. A. C. Brussee, A. Meetsma, P. T. van Duijnen, J. H. Teuben, *Organometallics* **1997**, *16*, 3511–3522.

[11] V. W.-W. Yam, K. M.-C. Wong, K.-K. Cheung, *Chem. Commun.* **1998**, 135–136.

[12] D. M. Tellers, J. C. M. Ritter, R. G. Bergmann, *Inorg. Chem.* **1999**, *38*, 4810–4818.

[13] a) E. Iravani, B. Neumüller, *Organometallics* **2003**, *22*, 4129–4135; b) W. Zarges, M. Marsch, K. Harms, G. Boche, *Angew. Chem.* **1989**, *101*, 1424–1425; *Angew. Chem. Int. Ed. Engl.* **1989**, *28*, 1392–1396; c) I. Langlotz, M. Marsch, K. Harms, G. Boche, *Z. Kristallogr.* **1999**, *509*, 214–217; d) J. R. Fulton, S. Sklenak, M. W. Bouwkamp, R. G. Bergman, *J. Am. Chem. Soc.* **2002**, *124*, 4722–4737; e) D. A. Culkin, J. F. Hartwig, *J. Am. Chem. Soc.* **2002**, *124*, 9330–9331.

[14] G. M. Sheldrick, SHELXS-97 Program for the Solution of Crystal Structures, Universität Göttingen (Germany), **1990**.

[15] G. M. Sheldrick, SHELXL-97 Program for the Refinement of Crystal Structures, Universität Göttingen (Germany), **1997**.

[16] G. M. Sheldrick, SADABS Program for Empirical Absorption Correction of Area Detector Data, Universität Göttingen (Germany), **1996**.

[17] A. L. Spek, PLATON A Multipurpose Crystallographic Tool, Utrecht University (The Netherlands) **2000**.

Received: March 24, 2005
Published online: July 20, 2005

